Flexible Graphene-Based Electroluminescent Devices

Ze-gao Wang,[†] Yuan-fu Chen,[†,*] Ping-jian Li,[†,*] Xin Hao, Jing-bo Liu, Ran Huang, and Yan-rong Li[*]

State Key Laboratory of Electronic Thin Films and Integrated Devices, University of Electronic Science and Technology of China, Chengdu 610054, China.
[†]These authors contributed equally to this work.

ABSTRACT For the first time, large-area CVD-grown graphene films transferred onto flexible PET substrates were used as transparent conductive electrodes in alternating current electroluminescence (ACEL) devices. The flexible ACEL device based on a single-layer graphene electrode has a turn-on voltage of 80 V; at 480 V (16 kHz), the luminance and luminous efficiency are 1140 cd/m^2 and 5.0 lm/W, respectively. The turn-on voltage increases and the luminance decreases with increasing stacked layers of graphene, which means the single-layer graphene is the best optimal choice as the transparent conductive electrode. Furthermore, it demonstrates that the graphene-based ACEL device is highly flexible and can work very well even under a very large strain of 5.4%, suggesting great potential applications in flexible optoelectronics.

KEYWORDS: graphene · electroluminescence devices · flexible optoelectronics · luminance · luminous efficiency

Lighting and display have emerged as two of the most rapidly developing technologies of the 21st century with the coming of a global energy crisis. Low processing costs and mechanical stretchability render flexible optoelectronic devices highly attractive for many applications. Graphene, a new two-dimensional, one atom thick nanomaterial with excellent transmittance and conductivity,[1,2] has initiated the development of graphene-based optoelectronics, such as liquid-crystal devices,[3] light-emitting devices,[4,5] touch-screen panels,[6] and solar cells.[7,8]

Alternating current electroluminescence (ACEL) devices have attracted great attention in areas of liquid-crystal display backlighting and large-scale architectural and decorative lighting,[9,10] which is due to their high resolution, good contrast and brightness, uniform light emission, thin profile, and low power consumption.[11] Compared with OLEDs and LEDs, ACEL is still the only mature technology for flat and flexible large-area light sources until now.[12] ACEL devices commonly use indium tin oxide (ITO) films as transparent conductive electrodes, whose brittle nature hinders the mechanical stretchability of ACEL devices.[13−15] In comparison to ITO films, graphene has superior optoelectronic properties, better flexibility, and chemically stability.[3,16,17] On the other hand, high-quality, large-area graphene films have been prepared on transition metals by chemical vapor deposition (CVD) methods.[17−19] So, CVD-grown graphene is an excellent candidate to replace ITO film in ACEL devices, especially in the case of flexibility.

In this study, for the first time, we demonstrate high-performance ACEL devices on flexible PET substrates based on graphene transparent electrodes. The ACEL device with a single-layer graphene electrode has a turn-on voltage of 80 V; at 480 V (16 kHz), the luminance and luminous efficiency are 1140 cd/m^2 and 5.0 lm/W, respectively. It can work very well even under a very large strain of 5.4%. In addition, we show that the turn-on voltage increases and the luminance decreases with increasing stacked layers of graphene; therefore, the single-layer graphene is the best optimal choice as the transparent conductive electrode for graphene-based ACEL devices.

RESULTS AND DISCUSSION

Figure 1 shows the schematic structures and photographs of an ACEL device based on a single-layer graphene electrode before and after bending. We used the graphene films on a PET substrate as the transparent conductive electrode, the mixture of ZnS:Cu powder and epoxy as the phosphor layer, the mixture of $BaTiO_3$ powder and epoxy as the insulating layer, and the silver paste as the back electrode. The ACEL emitted light when high electric field was applied to the phosphor layer, as shown in Figure 1.

In order to investigate the influence of graphene transparent electrode on the device performance, we first studied the optical and electrical properties of CVD-graphene films. Graphene films were synthesized on Cu foils by CVD method,

* Address correspondence to y.chen@uestc.edu.cn, lipingjian@gmail.com, yrli@uestc.edu.cn.

Received for review May 21, 2011 and accepted August 15, 2011.

Published online August 15, 2011
10.1021/nn2018649

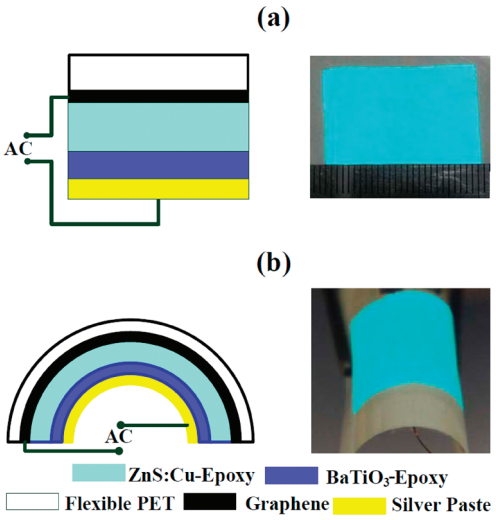

Figure 1. Schematic structures (left) and photographs (right) of ACEL device based on a single-layer graphene transparent electrode (a) before and (b) after bending; the device area is ~6 cm^2, and the applied voltage is 480 V.

which was similar to the previously reported process.[19] After growth, we used a PMMA layer as a support material to transfer large-area CVD-graphene film to a target substrate for further characterizations and measurements.[18,20] Figure 2a shows the Raman spectrum of the CVD-graphene transferred onto a 300 nm SiO_2/Si substrate. One can observe two peaks of graphene at ~1584 cm^{-1} (G peak) and ~2699 cm^{-1} (2D peak). The G-to-2D intensity ratio (I_G/I_{2D}) is ~0.28, which indicates the CVD-graphene is single layer.[19] In addition, the intensity of the D band at ~1350 cm^{-1}, a measure of defects in the graphene, is below the Raman detection limit, which means our CVD-graphene has high quality. We measured the optical and electrical properties of single and multiple stacked layer graphene films, which were transferred onto PET substrates. The multiple stacked layer graphene was obtained by using the transfer process sequentially, and the resulting films (~6 cm^2) are shown in Figure 2b.

Figure 2c shows the optical transmittance of graphene films on PET substrates as a function of wavelength for different numbers of stacked layers. From Figure 2c, we can obtain the transmittance of graphene as a function of the number of stacked layers at the wavelength of 497 nm (the inset in Figure 2c), which corresponds to the emission peak of our graphene-based ACEL devices. The transmittance of single-layer graphene is 96.3%, and the transmittance is reduced by ~3.37% by adding one layer of graphene, as similar to previous reports.[6,20] Figure 2d shows the sheet resistance of graphene films onto PET substrates. With the number of stacked layers (N) increasing from 1 to 4, the sheet resistance (R_N) decreases from 230 to 30 Ω/□. If the randomly stacked layers behave independent of each other, the average sheet resistance per layer (NR_N) should be constant; however, the actual value of average sheet resistance per layer decreases with increasing the stacked layers, as shown in Figure 2d (violet solid circle). The discrepancy may be explained by considering that the defects (or impurities) in one layer are bridged by its neighboring layer, and they increase with increasing the number of stacked layers. The defects (or impurities) may be produced during the transfer process. It is noted that the increase of defects (or impurities) has little influence on the optical transmittance of graphene films at normal incidence (the inset in Figure 2c) but will play an important role in optical transmittance at oblique incidence (Figure S1 in the Supporting Information).

Figure 3 shows the luminance of (unbending) ACEL devices based on 1−4 stacked layers of graphene as transparent electrodes. The turn-on voltage is defined as the voltage at which the luminance reaches 0.8 cd/m^2. One can observe that the turn-on voltage is 80 V (16 kHz) for the ACEL device based on a single-layer graphene electrode, and the value increases with increasing the number of stacked layers, as shown in the left top inset in Figure 3. The result is due to the following two reasons: (1) The increase of stacked layers does not influence the voltage drop of phosphor layer, which causes the occurrence of ACEL. It can be explained by the simple circuit model shown in the right bottom inset of Figure 3. The voltage drop of phosphor can be calculated from $U_{Phosphor} \approx U - U_{Graphene}$, where U is the applied voltage and $U_{Graphene}$ the voltage drop of graphene. $U_{Graphene}$ can be obtained by $U_{Graphene} = UR_{Graphene}/(R_{Graphene} + 1/2\pi fC_{total})$, where f is the frequency of applied voltage (16 kHz), C_{total} the total capacitance of the device (0.95 nF, measured by Agilent 4284), and $R_{Graphene}$ the resistance of graphene films. $R_{Graphene}$ is given by $R_{Graphene} = R_s t_f^2/S$, with R_s being the sheet resistance of graphene films (Figure 2d), t_f the thickness of graphene films, and S the area of graphene films (6 cm^2). When the number of stacked layers increased from 1 to 4, $\Delta U_{Phosphor}/U_{Phosphor} \approx \Delta U_{Graphene}/U \approx 5 \times 10^{-18}$. Therefore, the voltage of phosphor layer is independent of stacked layers. (2) The transmittance of graphene films (T_N) decreases with increasing stacked layers, as shown in the inset in Figure 2c. On the basis of these two reasons, we can conclude that, with increasing the number of stacked layers, the luminance decreases at the same applied voltage, thus the turn-on voltage correspondingly increases.

In order to further investigate the influence of the number of stacked layers on the luminance of devices, Figure 4a shows the luminance decay of the second layer ($(L_1 - L_2)/L_1$) as a function of applied voltage. One can observe that the luminance decay decreases with increasing applied voltage; when the applied voltage is beyond 320 V, the luminance decay reaches the saturation value of 6.1%, which is still higher than the transmittance decay value of the second layer ($(T_1 - T_2)/T_1 = 3.18\%$, normal

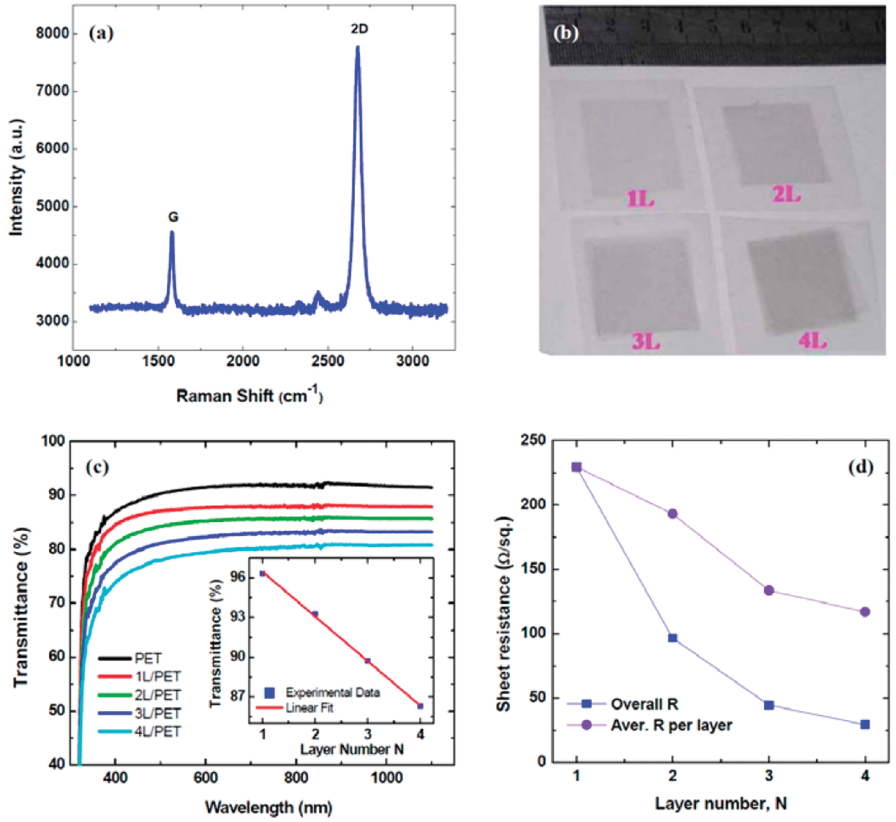

Figure 2. (a) Raman spectrum of the CVD-graphene transferred onto a 300 nm SiO_2/Si substrate. (b) Photographs of 1−4 layers of stacked graphene films on PET substrates; the film area is ~6 cm^2. (c) Transmittance of CVD-graphene films transferred on PET substrates for different numbers of stacked layers; the inset is the transmittance of graphene as a function of the number of stacked layers at the wavelength of 497 nm. (d) Sheet resistance of *N*-layer graphene as a function of the number of stacked layers (*N*).

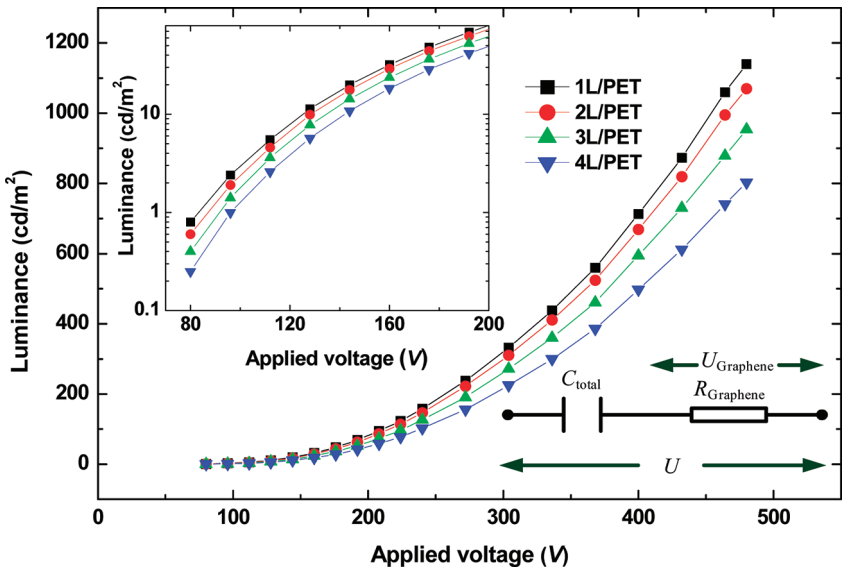

Figure 3. Luminance of ACEL devices based on 1−4 stacked layers of graphene as transparent electrodes, and the device area is ~6 cm^2. The left top inset is a semilog plot when applied voltage is smaller than 200 V, and the right bottom inset is the simple circuit model of the ACEL device.

incidence). The result may be mainly due to the surface relief of $BaTiO_3$-epoxy (at the silver paste/$BaTiO_3$-epoxy interface), which originated from the spin-coating process. As shown in Figure 4b, the surface relief of the $BaTiO_3$-epoxy layer on the phosphor layer is micrometer scale. It causes the non-uniform electric-field intensity and direction

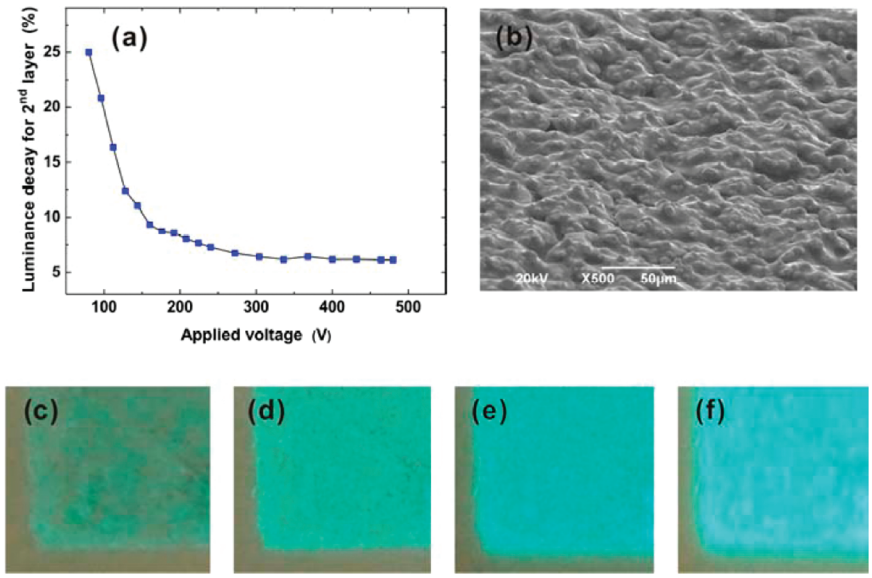

Figure 4. (a) Luminance decay of the second layer (($L_1 - L_2$)/L_1) as a function of applied voltage. (b) SEM image of $BaTiO_3$-epoxy on ZnS:Cu-epoxy/graphene/PET. (c−f) Photographs of the ACEL devices at various voltages of 120, 160, 240, and 320 V, respectively.

in the phosphor layer, resulting in the non-uniformity in intensity and direction of excited light. When the applied voltage is small, the ACEL first occurs at the concave parts of phosphor layer due to the formation of higher electrical field; in this case, the light is obliquely incident to the graphene films, which causes the lower transmittance than that at normal incidence.[21] When the applied voltage is increased, the luminous points increase; in this case, the more flat parts begin to glow, and the corresponding light is normally incident to the graphene films which causes the higher transmittance, thus the luminance decay is decreased. When the applied voltage is high enough, all parts of phosphor layer begin to glow; in this case, the luminance decay reaches the saturation value. This model can be supported by the photographs of the ACEL device at different applied voltage, as shown in Figure 4c−f; there are a few luminous points with a non-uniformly distributed state under small voltage, and the number of luminous points increases with increasing the applied voltage.

Moreover, at the applied voltage of 480 V, the luminance decays of the second, the third, and the fourth layer are 6.1, 10.8, and 15.8%, respectively, as shown in Figure S1 (Supporting Information). The luminance decay of the *N*th layer (($L_{N-1} - L_N$)/L_{N-1}) graphene increases with increasing the layer number (*N*). It may be due to the defects (or impurities) of the *N*th layer increasing with the number of stacked layers, resulting the increase of scattering effects.[22] Figure S2a−d shows the AFM images of 1−4 layers of stacked graphene films on PET substrates, respectively. One can observe that, when the stacked layers increase from 1 to 4, the defects and impurities increase, and the corresponding root-mean-square (rms) roughness increases from 15.0 to 25.1 nm. It can be due to the random multilayer stacking, which introduces defects and impurities during every transfer process. Thus, the defects and impurities of the *N*th layer, originated from the (*N*−1)th layer and the *N*th transfer process, increase with the number of stacked layers. The result is also consistent with the electrical results, as shown in Figure 2d.

On the basis of the above studies, we conclude that the single-layer graphene is the best optimal choice as the transparent conductive electrode for graphene-based ACEL device, which has a turn-on voltage of 80 V. At 480 V (16 kHz), the luminance and luminous efficiency are 1140 cd/m^2 and 5.0 lm/W, respectively. The luminous efficiency of 5.0 lm/W was measured using a Sawyer−Tower circuit, as shown in Supporting Information Figure S3. The values are comparable to the common ACEL devices (ZnS:Cu phosphor layer),[23] and the device performance can be further improved by increasing the smoothness of $BaTiO_3$-epoxy layer (and ZnS:Cu-epoxy) surface.

In addition, we have also investigated the flexibility of ACEL device based on a single-layer graphene as the transparent electrode. As shown in Figure 5a, the strain is defined as strain $\approx (t_s - t_p)/2r_c$ (t_s, $t_p \gg t_f$), where t_s is the thickness of the substrate, t_p the total thickness of the phosphor layer, dielectric layer, and silver electrode, t_f the thickness of the graphene film, and r_c the curvature radius. Both the sheet resistance of single-layer graphene and the luminance of the ACEL device remain almost unchanged even when the strain increases to 5.4%, as shown in Figure 5b. Pleases note that the photograph of the bending graphene-based ACEL device is shown in Figure 1b. On the other hand, when the stain is greater than 2.5%, the resistance of ITO film (105 nm, 80 Ω/□) increases sharply, caused by the rapid increase of crack density with increasing

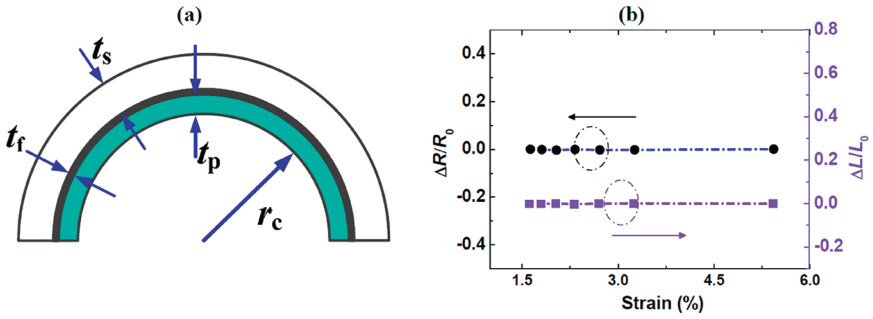

Figure 5. (a) Schematic structure of a bending graphene-based ACEL device; t_s is the thickness of the PET substrate; t_f is the thickness of graphene film; t_p is the total thickness of the phosphor layer, dielectric layer, and silver electrode; r_c is the radius of curvature. (b) Changes of sheet resistance and luminance as a function of strain; the black solid circles and violet solid squares represent the changes of sheet resistance and luminance (at 480 V), respectively; the photograph of the bending graphene-based ACEL device is shown in Figure 1b.

strain, as shown in Supporting Information Figure S4.[24] It is noted that, for the ACEL device, the increase in sheet resistance of ITO film has little influence on the voltage of the phosphor layer (ITO: $\Delta R/R_0 = 200 \rightarrow \Delta U_{Phosphor}/U_{Phosphor} \approx 2.8 \times 10^{-11}$), but the cracks will obviously influence the uniformity of luminance and decrease the life cycle of the device (typically for repeated bending).[6,24] So we conclude that the single-layer graphene has great advantage over ITO films for flexible ACEL devices.

CONCLUSIONS

In summary, for the first time, we have demonstrated the fabrication and performance of flexible ACEL devices based on graphene transparent electrodes. The influence of graphene transparent electrode on device performance was systemically studied. The results show that the turn-on voltage increases, and the luminance decreases with increasing stacked layers of graphene. It means that the single-layer graphene is the best optimal choice as the transparent conductive electrode for a graphene-based ACEL device, which has a turn-on voltage of 80 V. At 480 V (16 kHz), the luminance and luminous efficiency are 1140 cd/m^2 and 5.0 lm/W, respectively. Furthermore, we have also investigated the flexibility of graphene-based ACEL devices. Both the sheet resistance and luminance of the device remain unchanged under a large strain of 5.4%. The result reveals that flexible graphene-based ACEL devices will play an important role in flexible optoelectronics and have great potential in architectural and decorative lighting (*e.g.*, billboards, signs) or wearable devices (*e.g.*, wearable lighting, wearable displays).

METHODS

Graphene Synthesis. Graphene film with a size of 10 × 10 cm^2 was grown on 25 μm thick Cu foils (Alfa Aesar, item no. 13382) by CVD. The detailed growth process is very similar to that reported in ref 19. First, we loaded the Cu foil into the silica tube of the CVD system, then evacuated the system and backfilled with hydrogen; increased the temperature to 1000 °C within 40 min with a hydrogen flux of 30 sccm and pressure of 100 Pa; grew graphene films for 20 min by introducing 50 sccm of CH_4; and finally cooled the system to room temperature with a cooling rate of 50 °C/min.

Transfer Process of Graphene Films. The surface of the graphene-on-Cu was spin-coated with poly(methyl methacrylate) (PMMA), and the PMMA/graphene/Cu foil was baked on a hot plate at 100 °C for 3 min and then 120 °C for 5 min. Then the Cu foil was etched in an aqueous solution of 10 wt % $Fe(NO_3)_3$. After the Cu foil was completely etched, the PMMA/graphene was washed in DI water several times to remove Fe^{3+} and NO_3^-. The PMMA/graphene was transferred onto a flexible PET substrate (or SiO_2/Si substrate). In order to prevent the formation of bubbles between the graphene and PET substrate, the PMMA/graphene/PET was baked on a hot plate at a low temperature of 50 °C for 20 min. In order to prevent causing damages to large-area graphene, the acetone vapor instead of acetone solution was used to remove the PMMA, and the flexible graphene film on the PET was finally obtained.

Fabrication of ACEL Devices. First, the mixture of ZnS:Cu powder and epoxy with a weight ratio of 1.8:1 was spin-coated onto the graphene/PET, and it was baked at 110 °C for 30 min. The amount of Cu activator in the phosphor is around 0.1 wt % ZnS, and the size of ZnS:Cu powder is around 4−10 μm. The epoxy is AB glue purchased from Shanghai KPT Co. Then, the mixture of $BaTiO_3$ (10−15 μm) and epoxy (AB glue) with a weight ratio of 1:1 was spin-coated onto ZnS:Cu-epoxy/graphene/PET, and it was baked at 110 °C for 30 min. Finally, the silver paste electrode was coated, and the flexible ACEL device with a structure of silver paste/$BaTiO_3$-epoxy/ZnS:Cu-epoxy/graphene/PET was obtained, as schematically shown in Figure 1a. The thicknesses of ZnS:Cu-epoxy, $BaTiO_3$-epoxy, and silver paste electrode are about 100, 80, and 5 μm, respectively.

Measurements. All measurements were performed in air at room temperature. Raman spectroscopy was carried out on a Renishaw (514 nm). The optical transmittance was measured by using a Perkin-Elmer Model Lambda 750-UV−vis spectrophotometer. The sheet resistance of graphene was measured by Agilent 4155B using Van Der Pauw method. The luminance of ACEL was measured using a calibrated broad-band optical luminance meter (ST-86LA-3, Photoelectric Instrument Co, Beijing Normal University, China), and the luminance of a bent device was measured by putting the detector on the surface of bent PET. The capacitance of ACEL was tested by Agilent 4284.

Acknowledgment. We thank the financial support by the Program for New Century Excellent Talents in University, the Special Fund for Basic Scientific Research of Central Colleges,

University of Electronic Science and Technology of China (UESTC) and the startup research project of UESTC.

Supporting Information Available: Luminance decay of the second, third, and fourth layer at 480 V, AFM images of 1−4 layers of stacked graphene films on PET substrates, charge density *versus* voltage (*Q*−*V*) of graphene-based ACEL device, change in sheet resistance of ITO film on PET as a function of strain, and optical micrographs of ITO film on PET under strain. This material is available free of charge *via* the Internet at http://pubs.acs.org.

REFERENCES AND NOTES

1. Novoselov, K. S.; Geim, A. K.; Morozov, S. V.; Jiang, D.; Zhang., Y.; Dubonos, S. V.; Grigorieva, I. V.; Firsov, A. A. Electric Field Effect in Atomically Thin Carbon Films. *Science* **2004**, *306*, 666–669.
2. Geim, A. K.; Novoselov, K. S. The Rise of Graphene. *Nat. Mater.* **2007**, *6*, 183–191.
3. Blake, P.; Brimicombe, P. D.; Nair, R. R.; Booth, T. J.; Jiang, D.; Schedin, F.; Ponomarenko, L. A.; Morozov, S. V.; Gleeson, H. F.; Hill, E. W.; Geim, A. K.; Novoselov, K. S. Graphene-Based Liquid Crystal Device. *Nano Lett.* **2008**, *8*, 1704–1708.
4. Wu, J. B.; Agrawal, M.; Becerril, H. A.; Bao, Z. N.; Liu, Z. F.; Chen, Y. S.; Peumans, P. Organic Light-Emitting Diodes on Solution-Processed Graphene Transparent Electrodes. *ACS Nano* **2010**, *4*, 43–48.
5. Matyba, P.; Yamaguchi, H.; Eda, G.; Chhowalla, M.; Edman, L.; Robinson, N. D. Graphene and Mobile Ions: The Key to All-Plastic, Solution-Processed Light-Emitting Device. *ACS Nano* **2010**, *4*, 637–642.
6. Bae, S. K.; Kim, H. K.; Lee, Y. B.; Xu, X. F.; Park, J. S.; Zheng, Y.; Balakrishnan, J.; Lei, T.; Kim, H. R.; Song, Y.; et al. Roll-to-Roll Production of 30-Inch Graphene Films for Transparent Electrodes. *Nat. Nanotechnol.* **2010**, *5*, 574–578.
7. Wang, X.; Zhi, L. J.; Müllen, K. Transparent, Conductive Graphene Electrodes for Dye-Sensitized Solar Cells. *Nano Lett.* **2008**, *8*, 323–327.
8. Yin, Z. Y.; Sun, S. Y.; Salim, T.; Wu, S. X.; Huang, X.; He, Q. Y.; Lam, Y. M.; Zhang, H. Organic Photovoltaic Devices Using Highly Flexible Reduced Graphene Oxide Films as Transparent Electrodes. *ACS Nano* **2010**, *4*, 5263–5268.
9. Park, J. H.; Lee, S. H.; Kim, J. S.; Kwon, A. K.; Park, H. L.; Han, S. D. White-Electroluminescent Device with ZnS:Mn, Cu, Cl Phosphor. *J. Lumin.* **2007**, *126*, 566–570.
10. Vlaskin, V. I.; Vlaskina, S. I.; Koval, O. Y.; Rodionov, V. E.; Svechnikov, G. S. Flexible Electroluminescent Panels. *Semicond. Phys., Quantum Electron. Optoelectron.* **2007**, *10* 16–20.
11. Tiwari, S.; Tiwari, S.; Chandra, B. P. Characteristics of A.C. Electroluminescence in Thin Film ZnS:Mn Display Devices. *J. Mater. Sci.: Mater. Electron.* **2004**, *15*, 569–574.
12. Bredol, M.; Dieckhoff, H. S. Materials for Powder-Based AC-Electroluminescence. *Materials* **2010**, *3*, 1353–1374.
13. Forrest, S. R. The Path to Ubiquitous and Low-Cost Organic Electronic Appliances on Plastic. *Nature* **2004**, *428*, 911–918.
14. Chen, Z.; Cotterell, B.; Wang, W.; Guenther, E.; Chua, S. A Mechanical Assessment of Flexible Optoelectronic Devices. *Thin Solid Films* **2001**, *394*, 201–205.
15. Kaempgen, M.; Duesberg, G. S.; Roth, S. Transparent Carbon Nanotubes Coatings. *Appl. Surf. Sci.* **2005**, *252*, 425–429.
16. Fang, J. F.; Matyba, P.; Edman, L. Light-Emitting Electrochemical Cells: The Design and Realization of Flexible, Long-Lived Light-Emitting Electrochemical Cells. *Adv. Funct. Mater.* **2009**, *19*, 2519–2526.
17. Kim, K. S.; Zhao, Y.; Jang, H.; Lee, S. Y.; Kim, J. M.; Kim, K. S.; Ahn, J. H.; Kim, P.; Choi, J. Y.; Hong, B. H. Large-Scale Pattern Growth of Graphene Films for Stretchable Transparent Electrodes. *Nature* **2009**, *457*, 706–710.
18. Reina, A.; Jia, X.; Ho, J.; Nezich, D.; Son, H.; Bulovic, V.; Dresselhaus, M. S.; Kong, J. Large Area, Few-Layer Graphene Films on Arbitrary Substrates by Chemical Vapor Deposition. *Nano Lett.* **2009**, *9*, 30–35.
19. Li, X. S.; Cai, W.; An, J.; Kim, S.; Nah, J.; Yang, D.; Piner, R.; Velamakanni, A.; Jung, I.; Tutuc, E.; *et al.* Large-Area Synthesis of High-Quality and Uniform Graphene Films on Copper Foils. *Science* **2009**, *324*, 1312–1314.
20. Li, X. S.; Zhu, Y. W.; Cai, W. W.; Borysiak, M.; Han, B. Y.; Chen, D.; Piner, R. D.; Colombo, L.; Ruoff, R. S. Transfer of Large-Area Graphene Films for High-Performance Transparent Conductive Electrodes. *Nano Lett.* **2009**, *9*, 4359–4363.
21. Wood, R. W. *Physical Optics*; MacMillan: New York, 1934; pp 409−411.
22. Schrage, C.; Kaskel, S. Flexible and Transparent SWCNT Electrodes for Alternating Current Electroluminescence Devices. *ACS Appl. Mater. Interfaces* **2009**, *1*, 1640–1644.
23. Vij, D. R.; Singh, N. *Luminescence and Related Properties of II-VI Semiconductors*; Nova Publishers: New York, 1998; pp 185−185.
24. Cairns, D. R.; Witte, R. P.; Sparacin, D. K.; Sachsman, S. M.; Paine, D. C.; Crawford, G. P. Strain-Dependent Electrical Resistance of Tin-Doped Indium Oxide on Polymer Substrates. *Appl. Phys. Lett.* **2000**, *76*, 1425–1427.